IEEE Access
Multidisciplinary | Rapid Review | Open Access Journal

Received June 6, 2018, accepted July 13, 2018, date of publication July 23, 2018, date of current version August 15, 2018.

Digital Object Identifier 10.1109/ACCESS.2018.2858442

A Dual-Band Frequency Reconfigurable MIMO Patch-Slot Antenna Based on Reconfigurable Microstrip Feedline

XIONGWEN ZHAO, (Senior Member, IEEE), AND SHARJEEL RIAZ
School of Electrical and Electronic Engineering, North China Electric Power University, Beijing 102206, China

Corresponding author: Sharjeel Riaz (sharjeelrz@gmail.com)

This work was supported in part by the Key Program of Beijing Municipal Natural Science Foundation under Grant 17L20052, in part by the Beijing Municipal Science and Technology Commission under Grant Z181100003218007, and in part by the National Nature Science Foundation of China under Grant 61771194.

ABSTRACT In this paper, a novel microstrip feedline-based dual-band frequency reconfigurable multiple-input multiple-output (MIMO) patch-slot antenna design is presented. The antenna has a planar structure and comprises four symmetrically placed rectangular patch antenna elements. A dual-purpose hexagonal-shaped defected ground structure (DGS) is introduced into the ground plane for antenna size reduction and isolation enhancement. The overall size of the antenna is compact with total substrate area of $120 \times 60 \times 1.6$ mm^3 and is printed on FR4 substrate. Varactor diodes are integrated within feedline to achieve frequency reconfigurability. The proposed antenna design exhibits a wide continuous dual frequency reconfigurable characteristic from 1.3 to 2.6 GHz with isolation of more than 12 dB for entire band. The proposed design is verified by presenting the simulation and measured results of S-parameters, radiation pattern, efficiency, and envelope correlation coefficient (ECC), and displaying good agreement. ECC of less than 0.2 between the ports is achieved. The compact size and dual-band frequency reconfigurable characteristics make the proposed design potential candidate for wireless handheld devices and other multiband MIMO applications.

INDEX TERMS Dual-band, defected ground structure (DGS), frequency reconfigurable, reconfigurable feedline, MIMO, patch antenna.

I. INTRODUCTION

With the ever-increasing congestion of electromagnetic spectrum, frequency reconfigurable antennas have gained remarkable recognition due to their ability to adjust the operating frequency band based on spectrum availability, and adapt themselves to the requirements of changing environment, thus raising the frequency spectrum usage efficiency. Moreover, frequency reconfigurable antennas have compact size, low cost, simple integration, provides wideband or narrow band operation, allows single-band or multi-band configurations and frequency selectivity capability to reduce the co-site interference and jamming [1], making them suitable for many future wireless communication applications. Frequency reconfigurability can be achieved by using switches either in radiating elements or in microstrip feedline. The use of reconfigurable feedline is of great importance in frequency reconfigurable antennas and MIMO antennas for getting different radiation characteristics and for achieving diversity. Moreover, reconfigurable feedline allows achieving reconfigurability without including active components on radiating structure of antenna, which reduces cost, losses and eliminates unwanted radiation interference from biasing lines on the mounted antennas [2]. Thus, frequency reconfigurable antennas with reconfigurable feedline are highly desirable for modern communication systems.

Patch antennas are attractive candidates for frequency reconfigurable systems due to their low cost, low profile and planar structure, light weight, fabrication simplicity and their ability to easily integrate with different electronic devices. Various frequency reconfigurable patch antennas with operating frequency band between 1.5 to 3.5 GHz have been reported in [3]–[9]. In these designs, frequency reconfigurability was achieved by integrating pin diodes [3]–[5], varactor diodes [6]–[8] or microelectromechanical systems (MEMS) switches [9] into the radiating structure. In [3] and [4], two frequency reconfigurable patch antennas that can

switch frequencies between 1.7 and 3.5 GHz were proposed. These designs employed patch element of size 18.3 × 29 mm^2. In [5], a pattern and frequency reconfigurable patch antenna that could operate at 2.43 and 3.3 GHz was reported. The size of single patch element was 36 × 30 mm^2. A u-slot based patch design was presented in [6]. It provides tunable frequency range from 2.6 to 3.35 GHz with patch element size of 57 × 77 mm^2. In [7], a dual-band stacked patch antenna with two square patches was employed to achieve frequency tunability from 1.68 to 1.93 GHz and from 2.11 to 2.51 GHz. The size of square patch was 82 × 82 mm^2. A patch-slot dual-band design with operating frequency band from 2.22 to 2.26 GHz and from 3.24 to 4.35 GHz was proposed in [8]. The size of square patch element was 38 × 38 mm^2. In [9], a frequency reconfigurable E-shaped patched antenna (FR-ESPA) was presented with frequency tuning range from 2 to 3.2 GHz. The size of patch element was 44.1 × 92.5 mm^2. Majority of the frequency reconfigurable patch antenna designs cited in literature use single patch antenna element and suffer from narrow bandwidth and large size. Moreover, these designs were not able to achieve frequency reconfigurability in dual-band using reconfigurable feedline and had limited frequency tuning range. Therefore, the focus of this paper was to design a frequency reconfigurable patch antenna with MIMO capability in compact size that is suitable for small wireless devices, such as tablets and smart phones. Furthermore, the proposed antenna employs reconfigurable feedline to achieve frequency reconfigurability in dual-band with wide range tunability.

Multiple-input multiple-output (MIMO) antennas improve the channel capacity and can provide higher data rates at same transmission power. Hence MIMO antennas are best suited for the fourth-generation (4G) cellular communication and cognitive radio systems. To combine the advantages from MIMO and frequency reconfigurable antennas, several frequency reconfigurable MIMO antenna designs have been reported in [10]–[12]. No four-port frequency reconfigurable MIMO antenna design based on patch-slot configuration appeared in literature. In [10], a two-port frequency reconfigurable MIMO antenna with miniaturized patch elements was presented for frequency range from 2.1 to 2.4 GHz. A two-port reconfigurable MIMO antenna with full metal rimmed design for smartphone applications in LTE/WWAN band was proposed in [11]. In [12], a four-port reconfigurable MIMO slot design was presented for WLAN applications. None of these designs employed reconfigurable feedline to obtain reconfigurability. To our knowledge, a four-port frequency reconfigurable MIMO antenna design based on patch-slot configuration has never been reported in literature that employed reconfigurable feedline to achieve frequency reconfigurability.

In this paper, a novel four-port frequency reconfigurable MIMO antenna with reconfigurable feedline is proposed. The proposed antenna design is different from previous frequency reconfigurable designs available in literature. Our contributions are as follows:

1. a novel feedline-based frequency reconfigurable patch antenna;
2. a novel four-element frequency reconfigurable patch antenna design working at 1.3-2.6 GHz band;
3. a novel frequency reconfigurable patch design with wide tuning range, namely 1.3 to 2.6 GHz and providing dual-band performance;
4. a compact single patch element having DGS in the ground plane with an area of 22 × 14 mm^2;
5. a compact overall design with size of 120 × 60 × 1.6 mm^3 while providing isolation greater than 12 dB.

The proposed design consists of four rectangular patch antenna elements with hexagonal-shaped DGS slot in ground plane. The DGS provides compactness to the design as well as improves the isolation between antenna elements. Two slots were inserted in each patch element for bandwidth enhancement. The antenna system provides dual-band frequency reconfigurable characteristics with tunable operating frequency range from 1.3 to 1.8 GHz for the lower band and from 1.8 to 2.6 GHz for the higher band. The antenna was made frequency reconfigurable by tuning varactor diode that was placed in microstrip feedline. The antenna size is compact with dimensions of 120 × 60 mm^2. Details of the proposed antenna design and its performance are described in the following sections of this paper.

II. ANTENNA DESIGN

A. ANTENNA CONFIGURATION

Fig. 1 describes the geometry of the proposed antenna with detailed dimensions. The top and bottom views are shown in Fig. 1. The antenna is printed on 1.6 mm thick FR4 substrate with relative permittivity of 4.4, loss tangent of 0.02 and overall dimensions of 120 × 60 mm^2. The antenna ground is the ground plane on bottom side of FR4 substrate. The ground plane size was 60 × 120 mm^2. The proposed design comprises of four rectangular-shaped patch antenna elements of same size and geometry, labeled as Ant1 - Ant4, placed around four edges of the substrate as shown in Fig. 1. The single patch antenna element size is 22 × 14 mm^2. Each antenna element is fed by 50 Ω microstrip line. Frequency reconfigurability is achieved by a reconfigurable microstrip feedline using varactor diodes. The varactor diodes are BBY65-02V where the capacitance of the diode changes from 35 to 2.5 pF when the reverse bias voltage increases from 0 to 5 V. Continuous dual frequency reconfigurable band was achieved by tuning the varactor diode reverse bias voltage.

B. SINGLE ELEMENT ANTENNA

Fig. 2 illustrates the design mechanism of a single antenna element of the four-port antenna. As a starting point, rectangular patch antenna element having dimension of 22 × 14 mm^2 on substrate board size of 22 × 14 mm^2 was chosen for the design as shown in Fig. 2(a). Proper impedance matching is important to achieve the optimum return loss at desired frequency This rectangular patch antenna element was fed by a 50 Ω microstrip line and impedance matching

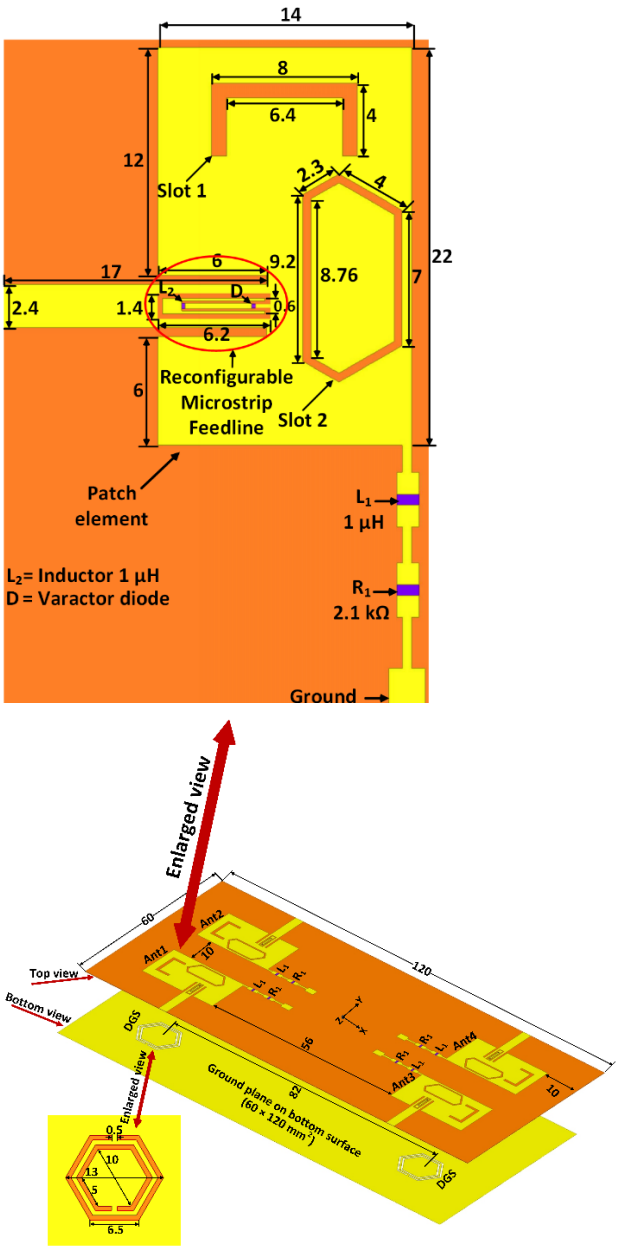

FIGURE 1. Geometry of the proposed four-port frequency reconfigurable MIMO antenna design. All dimensions are in mm.

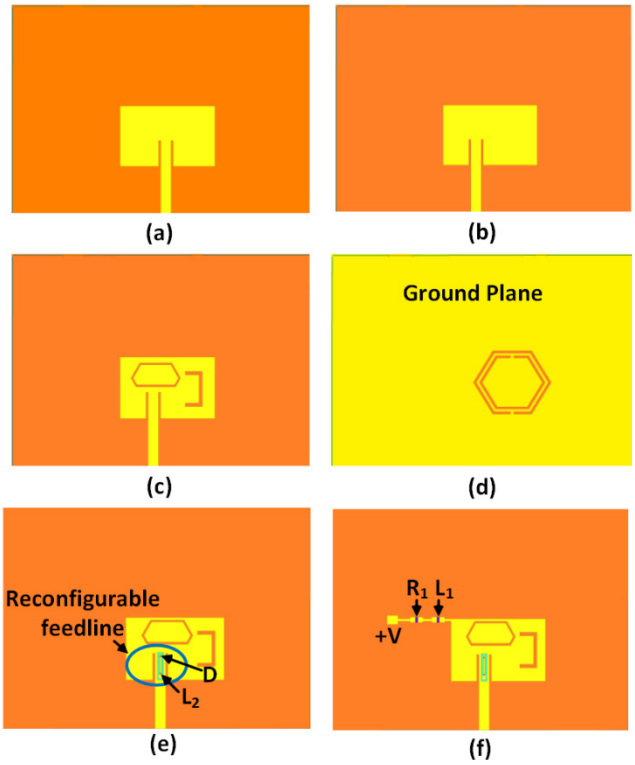

FIGURE 2. Steps involved during the single antenna element design procedure (a) Rectangular patch (b) Impedance matching (c) Introduction of slots (d) with DGS in ground plane (e) with reconfigurable feedline (f) with biasing network (final design).

between patch and transmission line was improved by varying the position of microstrip feedline as shown in Fig. 2(b). Patch antennas suffer from narrow bandwidth and large size which makes them unsuitable for modern wireless applications. Two slots were inserted in the patch element for bandwidth enhancement as shown in Fig. 2(c).

A defected ground structure (DGS) is used in antennas' ground plane for size reduction and isolation enhancement between antenna elements [13]. Normal patch antennas as shown in Figs. 2(a) and 2(b) resonate at frequencies around 3.5 GHz. In order to lower down the resonance frequency without increasing the antenna size, a hexagonal-shaped DGS was incorporated in the ground (GND) plane of the antenna structure as shown in Fig. 2(d). This lower the frequency band of operation to 2.95 GHz. The advantage of using DGS as a miniaturization technique is that antenna geometry remains simple and planar [14]. Further improvement in size reduction was achieved using reactive loading that brought the resonance frequency down to 2.6 GHz.

A simple 50 Ω microstrip feedline, which is consisted of an inductor and varactor diode, is used to achieve frequency reconfigurability as shown in Fig. 2(e). Varactor diode corresponding to feed 1 is labeled as D. The anode of the varactor diode was soldered to feedline while the cathode was connected with rectangular patch. A dual-band frequency reconfigurable performance with continuous tunability from 1.3 to 1.8 GHz (for the first band) and from 1.8 to 2.6 GHz (for second band) was achieved by tuning the varactor diode reverse bias voltage.

The bias network consisted of a series combination of resistor R_1 and inductor L_1 as shown in Fig. 2(f). The varactor diode was connected with variable voltage source through R_1 and L_1. The DC GND is provided through coaxial cable and shared the same GND plane using SMA connector. An inductor L_2 is used to block any DC from the coaxial cable. The values of different lumped elements used were $L_1 = L_2 = 1\ \mu$H and $R_1 = 2.1$ KΩ.

III. RESULTS AND DISCUSSION

The proposed four-port frequency reconfigurable MIMO antenna was fabricated as shown in Fig. 3. A 50 Ω microstrip feedline was used for feeding antenna elements, which was made reconfigurable by employing varactor diode.

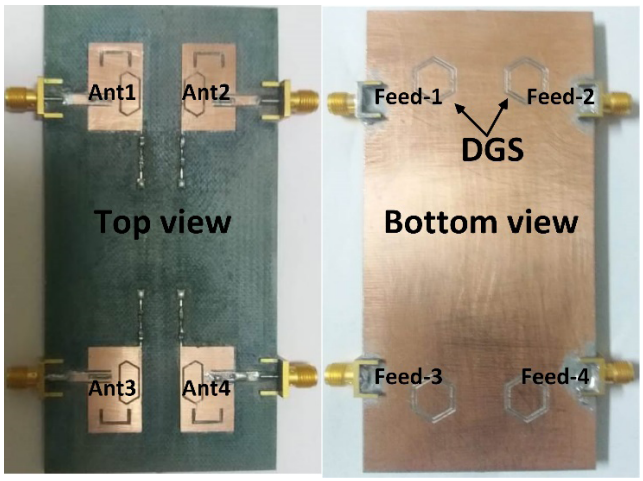

FIGURE 3. Fabricated frequency reconfigurable MIMO antenna.

A. S-PARAMETERS

Simulations using ANSYS HFSS were performed for S-parameters. Simulated S_{11} results in Fig. 4(a) shows that a dual-band is achieved with continuous frequency tunability from 1.3 to 1.8 GHz (for the lower band) and from 1.8 to 2.6 GHz (for the higher band), with −6 dB bandwidth of 45 MHz and 65 MHz respectively. The simulated operating frequency is obtained in HFSS by changing the capacitance value according to data sheet (35 to 2.5 pF). The dual-band is generated by the slots and DGS incorporation in the patch elements. The slots in the patch elements enhanced the bandwidth while with DGS, dual band was generated. The location of slots and DGS was critical in achieving optimum return loss with wide bandwidth and good isolation. To verify the simulation results, S-parameters were also measured using vector network analyzer. The measured reflection coefficient result in Fig. 4(b) shows that minimum −6 dB bandwidth of 50 MHz in the lower band (from 1.3 to 1.8 GHz) and 70 MHz in the the upper band (from 1.8 to 2.6 GHz) is achieved. The measured operating frequency is achieved by tuning reverse bias voltage of varactor diode from 0 to 5 V. The simulated and measured reflection coefficient results show good agreement. A slight shift in simulated and measured resonant frequency could be attributed to fabrication accuracy, soldering tolerances and parasitic effects in active and passive lumped components. Moreover, varactor diode's actual capacitance range is smaller compared to the datasheet.

Fig. 5 shows the mutual coupling results of the proposed four-port frequency reconfigurable MIMO antenna for different ports. The simulated and measured isolation results for other ports are not presented because of same dimensions

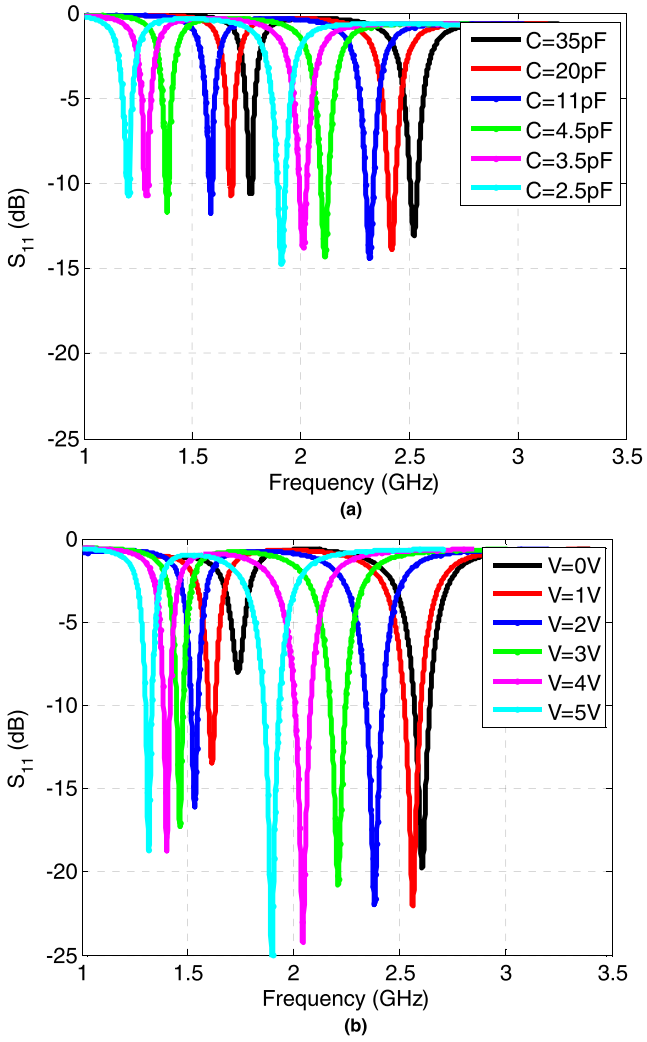

FIGURE 4. S-parameter results (a) simulated S_{11} (b) measured S_{11}.

and symmetric design of proposed antenna. Hence, we obtained similar results. To represent the effectiveness of DGS, the simulated S_{12} curves without and with DGS are shown in Figs. 5(a) and 5(b). It is evident that the introduction of DGS in the ground plane has greatly improved the mutual coupling between antenna elements.

Fig. 5 (c) shows the measured S_{12}. Simulated isolation curves, S_{13} and S_{14} are shown in Figs. 5(d) and 5(e). The minimum values observed for S_{13}, S_{14} were 15 dB and 20 dB, respectively, in the entire band of operation. The worst-case coupling was 8 dB at 2GHz without DGS structure between antenna 1 and 2, while with DGS it improved to at-least 12 dB. It is observed that mutual coupling for proposed four-port frequency reconfigurable MIMO design was enhanced 4 dB in the entire band of interest.

B. RADIATION PATTERNS AND EFFICIENCY

Fig. 6 shows the simulated and measured 2-D radiation patterns of the proposed four-port antenna at resonant frequency of 2 GHz placed in x-z ($\phi = 0°$) and y-z ($\phi = 90°$) plane.

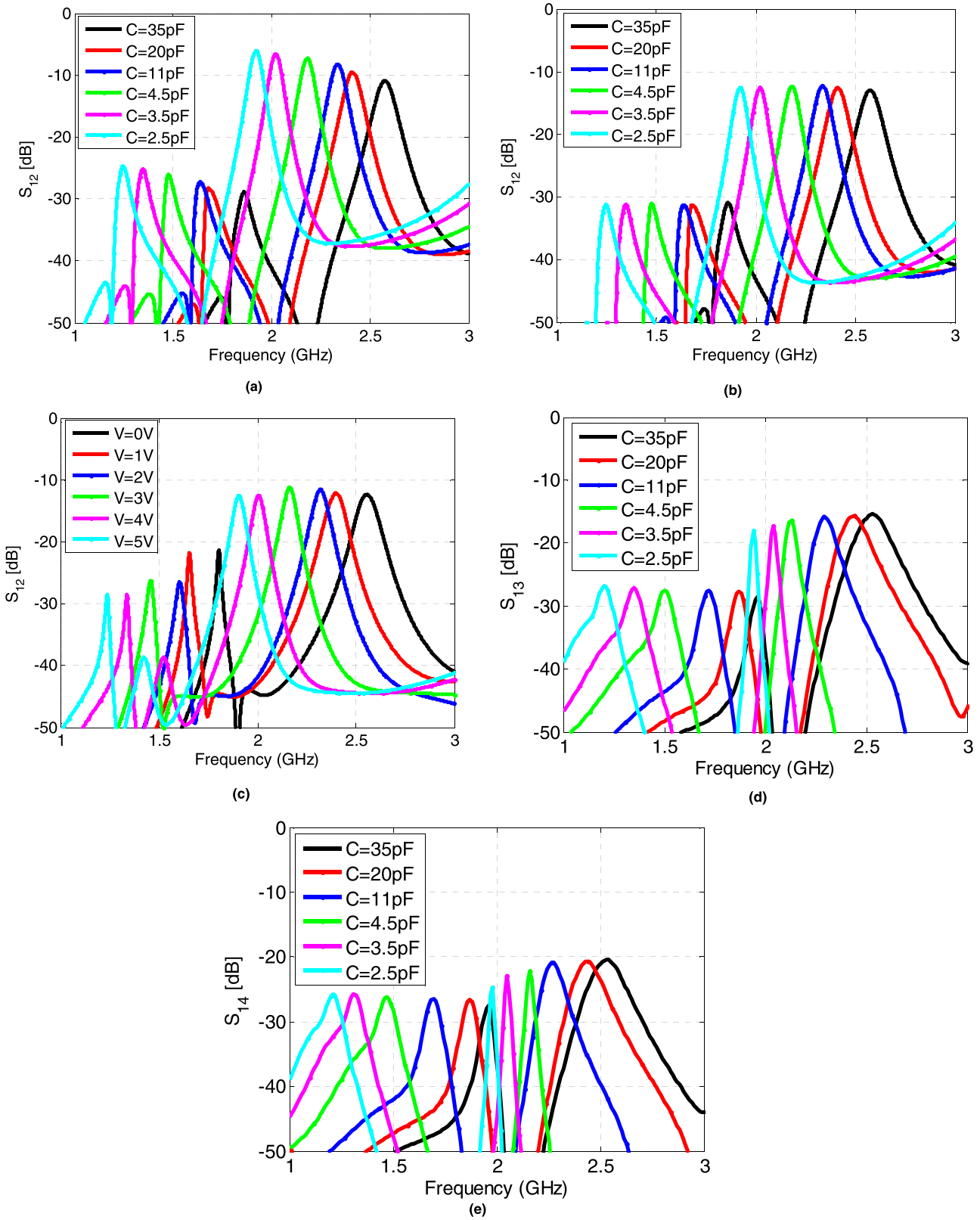

FIGURE 5. Mutual coupling results (a) simulatedS_{12} without DGS (b) simulated S_{12} with DGS (c) measured S_{12} (d) simulated S_{13} (e) simulated S_{14}.

Simulated and measured results show good agreement. The measurement was conducted with only one port excited and rest terminated to 50-Ω loads. The measured co-polarization and cross-polarization radiation patterns for the four antennas at 2GHz are shown in Fig. 7. These patterns are also compared in *x-z* and *y-z* plane. It was observed that the

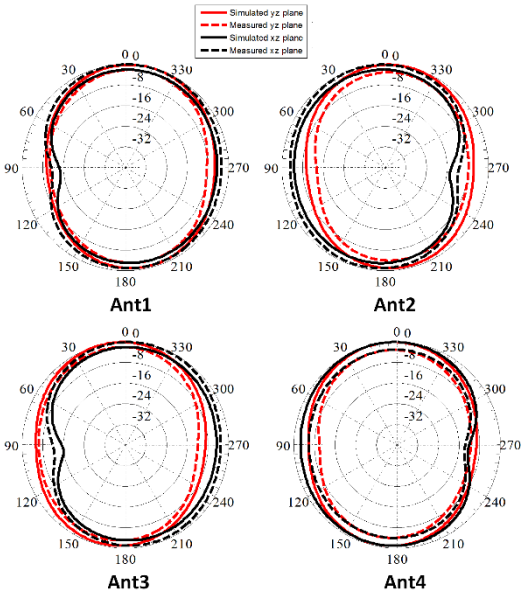

FIGURE 6. Simulated and measured radiation patterns of antenna elements in *x-z* and *y-z* planes at 2 GHz.

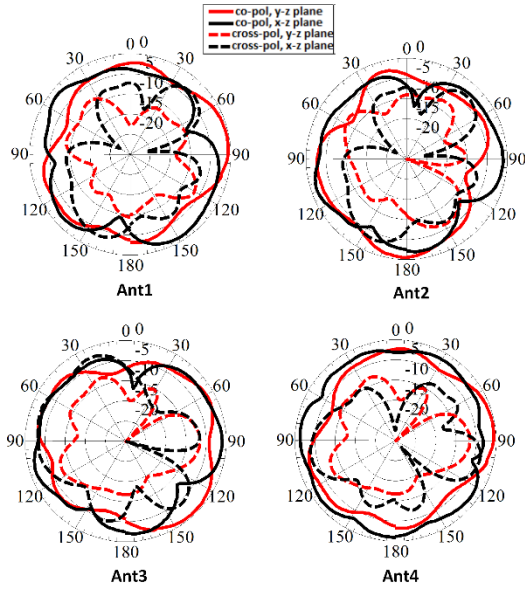

FIGURE 7. Measured co and cross-pol radiation patterns of antenna elements in x-z and y-z planes at 2 GHz.

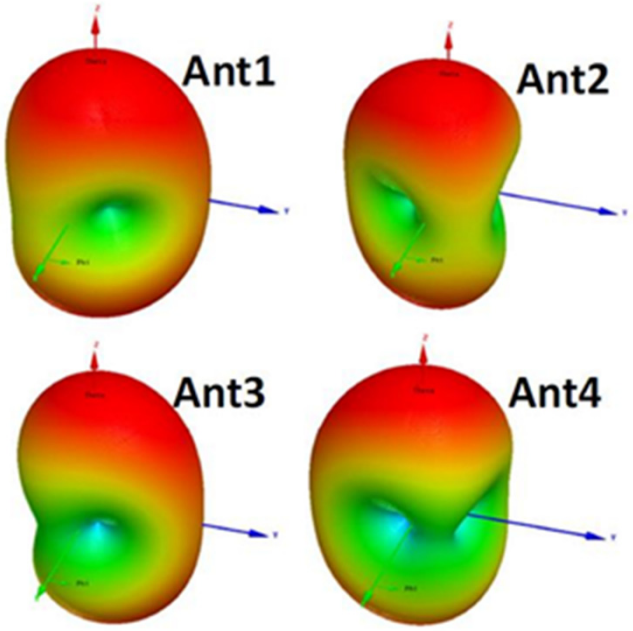

FIGURE 8. Simulated 3-D radiation patterns of antenna elements at 2 GHz.

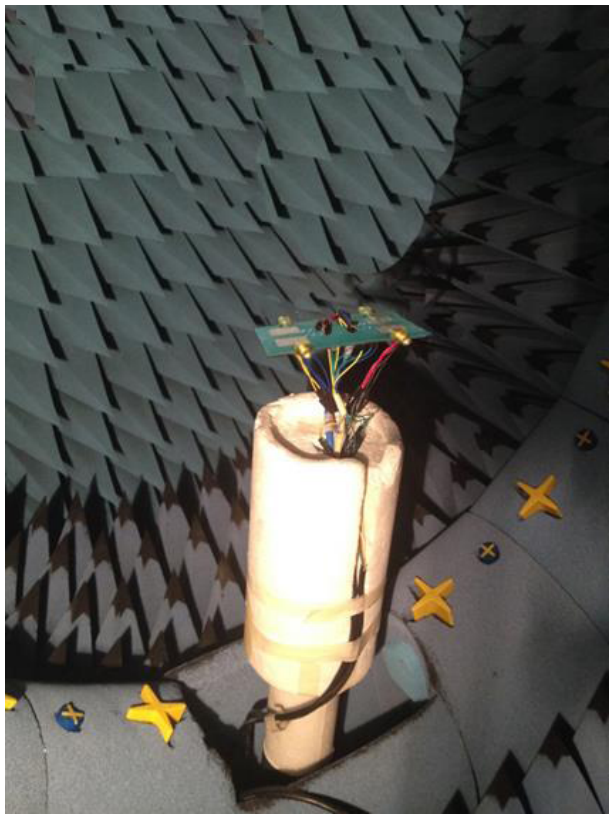

FIGURE 9. Setup for antenna radiation pattern measurement.

measured antenna gain varies from −1.9 to 2.48 dBi with peak efficiency of 78 %. The maximum gain is 2.48 dBi with efficiency of 72 % at 2.61 GHz and lowest gain is −1.9 dBi with efficiency of 48 % at frequency of 1.74 GHz. To further support the radiation pattern performance of the proposed antenna design, 3-D radiation patterns at 2 GHz from HFSS are shown in Fig. 8. The setup for antenna radiation pattern measurement is shown in Fig. 9.

Table 1 summarizes the proposed antenna performance characteristics such as simulated and measured bandwidth, gain and efficiency. The small difference between simulated and measured results is due to improper modeling of varactor diode in HFSS, parasitic effects of diode, manufacturing and

TABLE 1. Summary of antenna performance.

Sim. center freq., GHz Band 1/Band 2	1.763/ 2.52	1.672/ 2.417	1.578/ 2.311	1.387/ 2.107	1.289/ 2.011	1.199/ 1.907
Meas. center freq., GHz Band 1/Band 2	1.736/ 2.611	1.61/ 2.562	1.535/ 2.384	1.464/ 2.212	1.398/ 2.041	1.314/ 1.893
Sim. B.W, MHz ($\|S_{11}\|\leq$ -6dB) Band 1/Band 2	52/ 115	53/ 112	55/ 110	58/ 105	60/ 102	62/ 100
Meas. B.W, MHz ($S_{11}\|\leq$ -6dB) Band 1/Band 2	42/ 100	45/ 94	49/ 86	52/ 84	60/ 78	62/ 72
Sim. effi., % Band 1/Band 2	52/ 78	53/ 75	55/ 72	58/ 70	60/ 69	62/ 68
Meas. effi., % Band 1/Band 2	48/ 72	50/ 68	51/ 78	54/ 76	56/ 75	60/ 72
Sim. Gain, dBi Band 1/Band 2	-1.2/ 2.65	-0.8/ 2.55	-0.2/ 2.35	0.6/ 2.13	1.2/ 2.10	1.6/ 2.01
Meas. Gain, dBi Band 1/Band 2	-1.9/ 2.48	-1.8/ 2.39	-1.2/ 2.29	-0.6/ 2.01	0.2/ 1.86	1.1/ 1.75

TABLE 2. Simulated and measured ECC of the proposed antenna.

Mode	ECC for Band-1				ECC for Band-2			
Res.	Freq. (GHz)	Port 1,2	Port 1,3	Port 1,4	Freq. (GHz)	Port 1,2	Port 1,3	Port 1,4
Sim.	1.763	0.1629	0.1834	0.1138	2.52	0.0487	0.0572	0.0939
Meas.	1.736	0.1466	0.1651	0.1024	2.611	0.0438	0.0515	0.0845
Sim.	1.672	0.1859	0.1514	0.0024	2.417	0.07	0.1507	0.0674
Meas.	1.61	0.1673	0.1363	0.0021	2.562	0.063	0.1357	0.0607
Sim.	1.578	0.0393	0.0761	0.0324	2.311	0.0502	0.1136	0.1589
Meas.	1.535	0.0354	0.0685	0.0292	2.384	0.0452	0.1022	0.143
Sim.	1.387	0.1232	0.0152	0.0622	2.107	0.0947	0.0108	0.1057
Meas.	1.464	0.1109	0.0137	0.056	2.212	0.0852	0.0097	0.0951
Sim.	1.289	0.0703	0.1062	0.0331	2.011	0.1662	0.1558	0.1204
Meas.	1.398	0.0633	0.0955	0.0298	2.041	0.1495	0.1403	0.1084
Sim.	1.199	0.1171	0.1868	0.0526	1.907	0.1099	0.026	0.1308
Meas.	1.314	0.1053	0.1681	0.0473	1.893	0.099	0.0234	0.1177

measuring tolerances. These results suggest that the presented dual-band antenna has good performance over the whole operating band.

C. ECC

An envelope correlation coefficient (ECC) is a measure of how the MIMO channels are correlated and it directly affect the channel capacity which is an important aspect for MIMO. ECC is most commonly calculated using radiation patterns. The ECC (ρ_e) can be calculated using radiation patterns of two antennas as follows [15]:

$$\rho_e = \frac{\left|\iint_{4\pi}\left[\vec{F}_1(\theta,\emptyset)\cdot\vec{F}_2(\theta,\emptyset)\right]d\Omega\right|^2}{\iint_{4\pi}\left|\vec{F}_1(\theta,\emptyset)\right|^2 d\Omega \iint_{4\pi}\left|\vec{F}_2(\theta,\emptyset)\right|^2 d\Omega} \quad (1)$$

Where $\vec{F}_i(\theta,\phi)$ is the radiation pattern associated with i antenna element, with all other ports terminated with source impedance and $\cdot$ denotes the Hermitian product.

Table 2 shows the simulated and measured ECC results calculated between different antenna elements using radiation patterns. For a good diversity gain performance of MIMO antenna, ECC should be less than 0.5 [15]. As shown in Table 2, ECC was calculated for different frequencies for both bands. The worst ECC value was $ECC_{13} = 0.187$ and it occurs at 1.19 GHz. ECC is less than 0.2 across the entire operating band indicating that the proposed four-port frequency reconfigurable MIMO antenna achieves a good diversity performance over the entire tuning range by satisfying the ECC < 0.5 criterion for MIMO antenna.

IV. CONCLUSION

This paper presents a novel dual-band, four-port frequency reconfigurable MIMO antenna which is based on reconfigurable microstrip feedline. It provides wide frequency reconfigurable tuning range from 1.3 to 2.6 GHz with dual-band characteristics. Frequency reconfigurability is achieved in

dual-band by varactor diode tuning present in feedline. The antenna structure is composed of four slot-fed rectangular patch elements with hexagonal-shaped DGS in ground plane. The main benefits of proposed antenna structure include compact overall size (120×60 mm^2), low profile, low cost, planar structure, no radiation interference from biasing lines and easy fabrication. Overall isolation of more than 12 dB is achieved between all ports. The simulated and measured results show that proposed antenna exhibits frequency reconfigurability in dual-band with wide range tunability, provides stable radiation patterns and low ECC values. Therefore, the proposed antenna system is well suited for modern wireless communication systems.

REFERENCES

[1] C. G. Christodoulou, Y. Tawk, S. A. Lane, and S. R. Erwin, "Reconfigurable antennas for wireless and space applications," *Proc. IEEE*, vol. 100, no. 7, pp. 2250–2261, Jul. 2012.

[2] Y. Tawk, J. Costantine, A. H. Ramadan, K. Y. Kabalan, and C. G. Christodoulou, "A reconfigurable feeding network," in *Proc. 8th IEEE Eur. Conf. Antennas Propag. (EUCAP)*, The Hague, The Netherlands, Apr. 2014, pp. 1534–1536.

[3] H. A. Majid, M. K. A. Rahim, M. R. Hamid, and M. F. Ismail, "Frequency reconfigurable microstrip patch-slot antenna with directional radiation pattern," *Prog. Electromagn. Res.*, vol. 144, pp. 319–328, 2014.

[4] H. A. Majid, M. K. A. Rahim, M. R. Hamid, N. A. Murad, and M. F. Ismail, "Frequency-reconfigurable microstrip patch-slot antenna," *IEEE Antennas Wireless Propag. Lett.*, vol. 12, pp. 218–220, 2013.

[5] M. S. Khan, A. Iftikhar, A.-D. Capobianco, R. M. Shubair, and B. Ijaz, "Pattern and frequency reconfiguration of patch antenna using PIN diodes," *Microw. Opt. Technol. Lett.*, vol. 59, no. 9, pp. 2180–2185, Sep. 2017.

[6] S.-L. S. Yang, A. A. Kishk, and K.-F. Lee, "Frequency reconfigurable U-slot microstrip patch antenna," *IEEE Antennas Wireless Propag. Lett.*, vol. 7, pp. 127–129, 2008.

[7] L. Ge, M. Li, J. Wang, and H. Gu, "Unidirectional dual-band stacked patch antenna with independent frequency reconfiguration," *IEEE Antennas Wireless Propag. Lett.*, vol. 16, pp. 113–116, 2016.

[8] A. Khidre, F. Yang, and A. Z. Elsherbeni, "A patch antenna with a varactor-loaded slot for reconfigurable dual-band operation," *IEEE Trans. Antennas Propag.*, vol. 63, no. 2, pp. 755–760, Feb. 2015.

[9] H. Rajagopalan, J. M. Kovitz, and Y. Rahmat-Samii, "MEMS reconfigurable optimized E-shaped patch antenna design for cognitive radio," *IEEE Trans. Antennas Propag.*, vol. 62, no. 3, pp. 1056–1064, Mar. 2014.

[10] A. Raza, M. U. Khan, R. Hussain, F. A. Tahir, and M. S. Sharawi, "A 2-element reconfigurable MIMO antenna consisting of miniaturized patch elements," in *Proc. IEEE Int. Symp. Antennas Propag. (APSURSI)*, Fajardo, Puerto Rico, Jun./Jul. 2016, pp. 655–656.

[11] Z.-Q. Xu, Y.-T. Sun, Q.-Q. Zhou, Y.-L. Ban, Y.-X. Li, and S. S. Ang, "Reconfigurable MIMO antenna for integrated-metal-rimmed smartphone applications," *IEEE Access*, vol. 5, pp. 21223–21228, 2017.

[12] S. Soltani, P. Lotfi, and R. D. Murch, "A port and frequency reconfigurable MIMO slot antenna for WLAN applications," *IEEE Trans. Antennas Propag.*, vol. 64, no. 4, pp. 1209–1217, Apr. 2016.

[13] Z. Mahlaoui, E. Antonino-Daviu, M. Ferrando-Bataller, H. Benchakroun, and A. Latif, "Frequency reconfigurable patch antenna with defected ground structure using varactor diodes," in *Proc. 11th IEEE Eur. Conf. Antennas Propag. (EUCAP)*, Paris, France, Mar. 2017, pp. 2217–2220.

[14] M. U. Khan, M. S. Sharawi, and R. Mittra, "Microstrip patch antenna miniaturisation techniques: A review," *IET Microw. Antennas Propag.*, vol. 9, no. 9, pp. 913–922, Jun. 2015.

[15] R. G. Vaughan and J. B. Andersen, "Antenna diversity in mobile communications," *IEEE Trans. Veh. Technol.*, vol. VT-36, no. 4, pp. 149–172, Nov. 1987.

XIONGWEN ZHAO (SM'06) received the Ph.D. degree (Hons.) from the Helsinki University of Technology (TKK), Finland, in 2002. From 1992 to 1998, he was the Director and a Senior Engineer with the Laboratory of Communications System Engineering, China Research Institute of Radiowave Propagation. From 1999 to 2004, he was a Senior Researcher and a Project Manager with the Radio Laboratory, TKK, where he was involved in the areas of multiple-input multiple-output (MIMO) channel modeling and measurements at 2, 5, and 60 GHz, and UWB. From 2004 to 2011, he was a Senior Specialist with Elektrobit (EB) Wireless Solutions, EB Corporation, Espoo, Finland. During 2004–2007, he was a Senior Researcher with the European WINNER Project, focused on MIMO channel modeling for 4G radio systems. From 2006 to 2008, he was involved in the field of wireless network technologies such as WiMAX and wireless mesh networks. From 2008 to 2009, he was involved in the mobile satellite communications for GMR-1 3G, DVB-SH RF link budget, and antenna performance evaluations. During 2010–2011, he was involved in the spectrum sharing and interference management between satellite and terrestrial local thermal equilibrium networks. He is currently a Professor of wireless communications with North China Electric Power University, Beijing. He is the Chair of the projects supported by the National Science Foundation of China, the Beijing Natural Science Foundation, and the State Key Laboratories and Industries on Channel Measurements, Modeling, and Simulations. He was a recipient of the IEEE Vehicular Technology Society Neal Shepherd Memorial Best Propagation Paper Award in 2014. He is a reviewer for the IEEE Transactions, Journals, Letters, and conferences. He served as a TPC Member, the Session Chair, and a Keynote Speaker for numerous international and national conferences.

SHARJEEL RIAZ received the B.S. degree in electrical engineering from the University of Engineering and Technology, Taxila, Pakistan, in 2006, and the M.Sc. degree in telecommunication engineering from the National University of Science and Technology, Pakistan, in 2009. He is currently pursuing the Ph.D. degree in electrical engineering with North China Electric Power University, Beijing, China. He was a Lecturer with the Electrical Engineering Department, Comsats Institute of Information Technology, Islamabad, Pakistan, where he was involved in various research projects and teaching. His research interests include design and analysis of multiple-input multiple-output antennas, reconfigurable antennas, and antennas for cognitive radio.